Quantum Necking in Stressed Metallic Nanowires

J. Bürki,[1,3] Raymond E. Goldstein,[1,2] and C. A. Stafford[1]

[1]*Department of Physics, University of Arizona, Tucson, Arizona 85721, USA*
[2]*Program in Applied Mathematics, University of Arizona, Tucson, Arizona 85721, USA*
[3]*Physikalisches Institut, Albert-Ludwigs-Universität, D-79104 Freiburg, Germany*

(Received 6 September 2002; revised manuscript received 14 July 2003; published 19 December 2003)

When a macroscopic metallic wire is subject to tensile stress, it necks down smoothly as it elongates. We show that nanowires with radii comparable to the Fermi wavelength display remarkably different behavior. Using concepts from fluid dynamics, a partial differential equation for nanowire shape evolution is derived from a semiclassical energy functional that includes electron-shell effects. A rich dynamics involving movement and interaction of kinks connecting locally stable radii is found, and a new class of universal equilibrium shapes is predicted.

DOI: 10.1103/PhysRevLett.91.254501 PACS numbers: 47.20.Dr, 61.46.+w, 68.35.Ja, 68.65.–k

It has recently become possible to image metal nanowires with subatomic resolution, and record their structural evolution in real time, using transmission-electron microscopy [1–5], thus opening the door to a world of nonlinear dynamical phenomena at the nanoscale. Heretofore, most information about the structure and dynamics of nanowires was obtained indirectly from transport and cohesive properties [6–10]. Classical molecular dynamics simulations [11–14] provide important insights into atomic structure and dynamics of nanowires, but cannot explain the observed stability [1,3,5] of long nanowires, which would be unstable classically under surface tension [15]. Quantum molecular dynamics can in principle study this stability, but has thus far been limited to systems too small to address such issues (e.g., single or double chains [16,17]).

By contrast, a nanoscale free-electron model [18–21] has proven successful in explaining the quantum suppression of the Rayleigh instability [20]. Here we extend this approach by developing a *dynamics* for a free-electron nanowire under the assumption that surface diffusion is a dominant process. This dynamics, of intrinsic interest in nonlinear science, explicitly includes quantum-size effects and allows the study of a broad range of dynamical processes (see Figs. 1–4): approach to equilibrium of a nanowire, propagation of an instability, and evolution of a wire under elongation/compression. Figure 1 shows how an initially random nanowire necks down to a universal shape, consisting of a central cylinder connected to contacts having the form of unduloids of revolution, providing a dynamical mechanism for the nanofabrication technique invented by Kondo and Takayanagi [1]. Figure 4 compares well to early experiments on gold nanocontacts [6,7], showing perfect correlation between force and conductance with steep conductance steps, and a hysteresis between elongation and compression.

The model of a nanowire consists of free electrons confined to an axisymmetric wire by a hard-wall potential [18]. The wire radius is $R(z, t)$ in the interval $[0, L]$ along the z axis, and periodic boundary conditions [23] are used to extend $R(z)$. In contrast to the classical case [15] for which all nonaxisymmetric distortions raise the energy, Jahn-Teller distortions that break axisymmetry of nanowires *do* lower the energy in a few cases. However, the deepest energetic minima occur for axisymmetric wires [24], and axisymmetry, once present, is preserved by the diffusion equation, so that Jahn-Teller distortions are most likely suppressed dynamically.

In the spirit of the Born-Oppenheimer approximation, the total energy of the nanowire is taken to be the

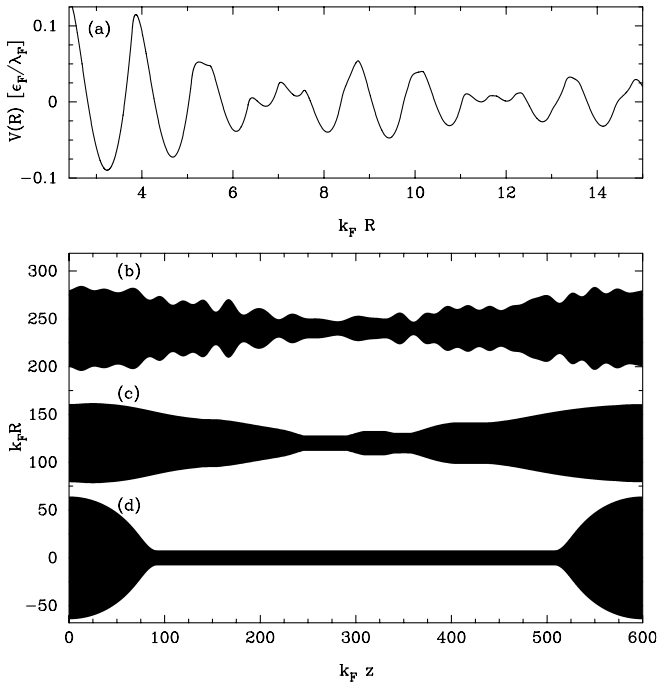

FIG. 1. (a) Electron-shell potential $V(T, R)$ for $T = 0.002T_F$. Here ε_F and λ_F are the Fermi energy and wavelength, $T_F = \varepsilon_F/k_B$ and $k_F = 2\pi/\lambda_F$. (b)–(d) Approach to equilibrium of an initially random wire [22]: (b) initial shape; (c) $\tau = 2 \times 10^4$; (d) $\tau = 3 \times 10^7$, equilibrium wire with $G = 12\,G_0$.

electronic energy. Since we are dealing with an open system of electrons, the grand-canonical potential is used, and can be separated into Weyl and mesoscopic contributions [19,25,26]. Dropping the volume contribution, which is assumed to be constant, the energy functional is

$$\Omega[T, R(z)] = \sigma(T) S[R(z)] + \int_0^L V[T, R(z)]\, dz, \qquad (1)$$

where $\sigma(T)$ is the surface tension [27], S is the surface area of the wire, and V is a mesoscopic electron-shell potential whose integral gives the so-called "shell correction" to the energy (as used, for instance, in the study of clusters [28]). Higher-order terms [19,26] proportional to the mean curvature, etc., are neglected. V can be expressed in terms of a Gutzwiller-type trace formula

$$V(T, R) = \frac{2\varepsilon_F}{\pi} \sum_{w=1}^{\infty} \sum_{\upsilon=2w}^{\infty} a_{\upsilon w}(T) \frac{f_{\upsilon w} \cos\theta_{\upsilon w}}{\upsilon^2 L_{\upsilon w}}, \qquad (2)$$

where the sum includes all classical periodic orbits (υ, w) in a disk billiard [26], characterized by their number of vertices υ and winding number w, $L_{\upsilon w} = 2\upsilon R \sin(\pi w/\upsilon)$ is the length of orbit (υ, w), and $\theta_{\upsilon w} = k_F L_{\upsilon w} - 3\upsilon\pi/2$. The factor $f_{\upsilon w} = 1$ for $\upsilon = 2w$, 2 otherwise, accounts for the invariance under time-reversal symmetry of some orbits, and $a_{\upsilon w}(T) = \tau_{\upsilon w}/\sinh\tau_{\upsilon w}$ $(\tau_{\upsilon w} = \pi k_F L_{\upsilon w} T/2T_F)$ is a temperature-dependent damping factor. A similar trace formula was previously derived [20] for small axisymmetric perturbations of a cylinder using semiclassical perturbation theory [26,29,30]. Here we point out that semiclassical perturbation theory remains valid for large deformations, as long as new classes of nonplanar orbits can be neglected (adiabatic approximation).

Equations (1) and (2) define an energy functional which is general and simple enough to solve for nontrivial nanowire geometries with a wide range of radii. The multiple deep minima of $V(R)$, shown in Fig. 1(a), favor certain magic radii [9] and suggest a multistable field theory analogous to the sine-Gordon model. We therefore anticipate solutions consisting of cylindrical segments connected by kinks.

Rather than directly minimizing the energy functional (1), we derive an equation describing the nanowire surface dynamics which yields the approach to equilibrium as well as the onset of instability. The model has two main assumptions. First, in the thin wires considered, the majority of atoms are at the surface and thus surface self-diffusion is the mechanism of ionic motion. Second, under the Born-Oppenheimer approximation, the electronic energy (1) acts as a potential for the ions, and the dynamics derive from ionic mass conservation:

$$\frac{\partial R(z,t)}{\partial t} = -\frac{\upsilon_a}{R(z,t)} \frac{\partial}{\partial z}[R(z,t) J_z(z,t)], \qquad (3)$$

where $\upsilon_a = 3\pi^2/k_F^3$ is the volume of an atom, and the z component of the surface current is given by Fick's law:

$$J_z = -\frac{\rho_S D_S}{k_B T} \frac{1}{\sqrt{1 + (R')^2}} \frac{\partial \mu}{\partial z}, \qquad (4)$$

where $R' = \partial R/\partial z$, and ρ_S and D_S are the surface density of ions and the surface self-diffusion coefficient, respectively. The precise value of D_S for alkali metals is not known, but it can be removed from the evolution equation by rescaling time to the dimensionless variable $\tau = (\rho_S D_S T_F/T)t$. The chemical potential μ is obtained by calculating the change in the energy (1) with the addition of an atom at point z_0, $\mu(z_0) \equiv \Omega[T, R(z) + A\delta(z - z_0)] - \Omega[T, R(z)]$, where $A = \upsilon_a/2\pi R$ is chosen so that the volume of an atom is added:

$$\mu(z) = -\frac{2\varepsilon_F}{5} + \frac{3\pi\sigma}{k_F^3 R(z)\sqrt{1 + R'^2}} \left(1 - \frac{RR''}{1 + R'^2}\right) - \frac{3\varepsilon_F}{k_F^2 R^2} \sum_{w,\upsilon} \frac{a_{\upsilon w} f_{\upsilon w}}{\upsilon^2} \left[\sin\theta_{\upsilon w} + b_{\upsilon w} \frac{\cos\theta_{\upsilon w}}{k_F L_{\upsilon w}}\right], \qquad (5)$$

where $b_{\upsilon w}(T) = a_{\upsilon w} \cosh\tau_{\upsilon w}$. Equation (3) is then solved numerically using an implicit scheme. Our nonlinear dynamical model, Eqs. (3)–(5), differs from previous studies of axisymmetric surface self-diffusion [31–33] by the inclusion of electron-shell effects [second line of Eq. (5)], which fundamentally alter the dynamics.

To explore the equilibrium shapes of nanowires, we considered several random initial configurations of various lengths and widths, one of which is shown in Fig. 1(b). Under surface self-diffusion, the short-wavelength fluctuations are rapidly smoothed out [Fig. 1(c)], and several cylindrical segments connected by "kinks" are visible. On a much longer time scale, the wires neck down to a universal equilibrium shape consisting of a nearly perfect cylindrical region with a radius near one of the minima of $V(R)$, connected to thicker leads [Fig. 1(d)]. In all 15 cases studied, the leads closely approximate Delaunay unduloids of revolution. The unduloid is a stationary

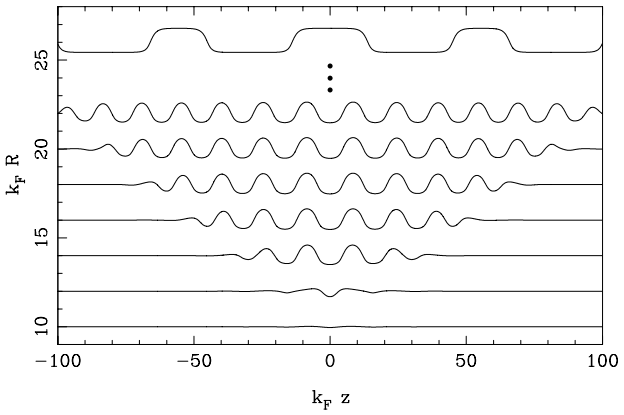

FIG. 2. Propagation of an instability [22] for a wire of initial radius $k_F R = 10$, time progressing from bottom to top ($\Delta\tau = 15$), with curves shifted for clarity. The top curve corresponds to a much later stage in the time evolution ($\tau = 6 \times 10^4$).

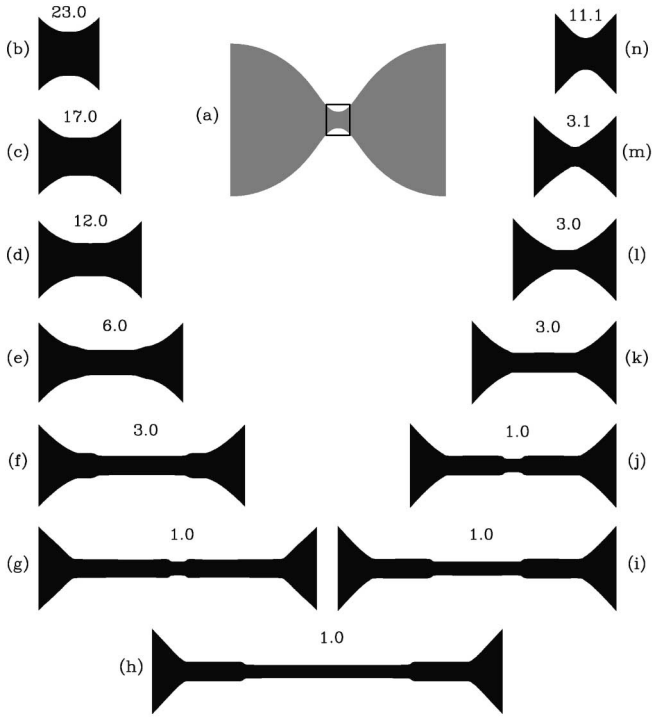

FIG. 3. Shape of a nanowire connecting two quasimacroscopic leads during elongation [left column, (b)–(h)] and subsequent compression [right column, (i)–(n)] [22]. For comparison, the entire system of length $L = 280k_F^{-1} + \Delta L$ is shown in inset [wire (a)], the small square indicating the nanowire shown in image (b). Adjacent wires have the same length, from top to bottom: $k_F\Delta L = 0$, 10, 20, 40, 70, 105, and 140. Above each wire is its conductance in units of G_0.

configuration, unstable under surface tension alone [33], but stabilized in the present model by electron-shell effects in the connecting cylinder. The unduloids arise as superpositions of large numbers of closely spaced kinks. Equilibrium wires with conductance $G/G_0 = 1, 3, 6, 12, 17, 23, \ldots$ were obtained, where $G_0 = 2e^2/h$ is the conductance quantum. Intermediate conductance values may occur more rarely.

Other cases of interest are the propagation of an instability [34] and the homogeneous-inhomogeneous transition in a nanowire [21]. In the former case, starting with a cylinder of an unstable radius, a maximum in $V(R)$ [Fig. 1(a)], and adding a localized Gaussian deformation of small amplitude ($0.001R$), we find that the perturbation decreases during an incubation period and then the instability sets in with essentially a single Fourier component corresponding to the most unstable mode [21], saturates at a finite amplitude, and propagates with constant velocity (see Fig. 2). A similar instability is observed in the pearling of membranes [35]. The classical Rayleigh instability itself [34] propagates in much the same way, but does not saturate, instead leading to breakup of the cylinder. Both the wavelength [21] and front velocity of the instability are strongly dependent on the initial radius. Once the instability is fully developed, kink-antikink pairs start annihilating, eventually leading to a shape consisting of a series of cylinders of different radii [corresponding to neighboring minima in $V(R)$, Fig. 1(a)], connected by kinks. Starting from a more realistic initial condition with random perturbations, the instability occurs at several places more or less simultaneously.

The dynamical model also allows for the study of the evolution of a nanowire under strain. The length L of the wire is changed at an average rate dL/dt in a sequence of infinitesimal steps. In each step, the wire deforms elastically, i.e., the change of length is distributed along the wire as if each of its slices were Hookean, with spring constant proportional to its cross-sectional area. The radius of each slice is simultaneously changed so as to conserve its volume. Between steps, the wire evolves according to Eq. (3). We start with an equilibrated unduloid of outer radius $k_F R = 99$, representing a nanocontact between two quasimacroscopic leads [see Fig. 3(a) (inset)]. We then strain the wire by elongating it at a constant speed $k_F dL/d\tau = 0.1$ until it necks down to a long, atomically thin wire [Fig. 3(b)–3(h)], at which point we let it partially equilibrate. Subsequently, we compress the wire at the same rate until it reaches its initial length [Fig. 3(i)–3(n)]. During elongation, the necking of the wire occurs by nucleation of kink-antikink pairs at the center with subsequent motion of these kinks toward the leads, leaving a long, cylindrical wire in the middle. During compression, the remaining kink-antikink pairs annihilate, but new kinks do not emerge from the leads. Similar necking was observed for various elongation rates $k_F dL/d\tau \leq 1$. For much faster rates, structural relaxation due to surface diffusion is suppressed.

These different processes lead to a substantial hysteresis between elongation and compression, as can be seen by computing the electrical conductance of the contact and the force applied to it. The force is obtained from the change in the energy (1) with elongation, $F = -\partial\Omega/\partial L$. The conductance is computed from the Landauer formula, using the adiabatic and WKB approximations [18] to compute the transmission probabilities. Both quantities are shown in Fig. 4. Compared to our previous results obtained without structural relaxation [18], the conductance steps and relaxations of the force are much steeper, in better agreement with experiments [6], and a substantial hysteresis is observed in the conductance. It has been argued [6,8] that the abruptness of the conductance steps, and their perfect correlation with the jumps in the force, rule out an electronic mechanism. However, we have shown that this behavior arises naturally in a model which takes proper account of electronic quantum-size effects on the structure, even when atomistic effects are neglected.

A final interesting feature is the spikes in the force that occur at the opening and closing of a channel, corresponding to the rapid energy relaxation during the creation or annihilation of a kink/antikink pair. These spikes

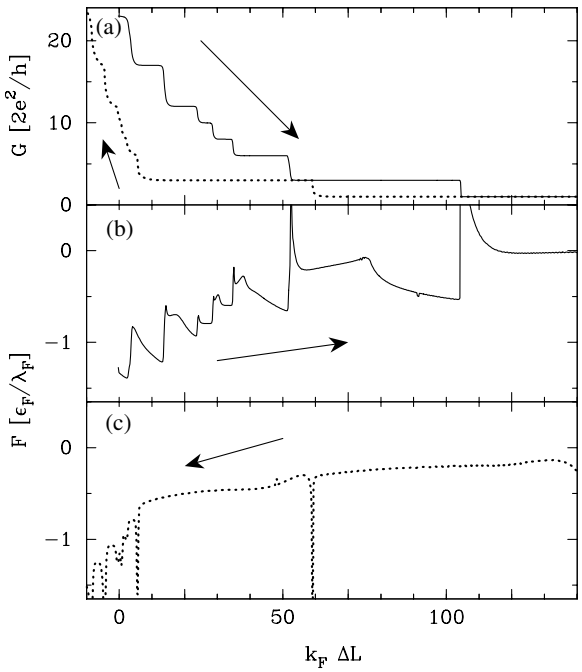

FIG. 4. Conductance and force as a function of ΔL for the wire of Fig. 3: (a) conductance during elongation (solid line) and compression (dotted line); (b) force during elongation; (c) force during compression.

are suppressed, and the hysteresis decreases, when the speed of deformation is increased, suggesting that the spikes might be observable experimentally by decreasing the elongation rate. A failure of this model is the force during compression: Contrary to experiment [6,8], the force is attractive, suggesting that a resistance to compression due to the ions needs to be added to the free-electron model. Indeed, an interesting question raised by this work is how discrete positive ions would arrange themselves to accommodate the predicted shapes favored by the conduction electrons.

This research was supported in part by NSF Grants No. DMR0072703 (J. B. and C. A. S.), No. DMR0312028 (C. A. S.), and No. DMR9812526 (R. E. G.). J. B. also acknowledges support from the Swiss National Science Foundation and Grant No. SFB276 of the Deutsche Forschungsgemeinschaft.

[1] Y. Kondo and K. Takayanagi, Phys. Rev. Lett. **79**, 3455 (1997).
[2] T. Kizuka, Phys. Rev. Lett. **81**, 4448 (1998).
[3] Y. Kondo and K. Takayanagi, Science **289**, 606 (2000).
[4] V. Rodrigues and D. Ugarte, Phys. Rev. B **63**, 073405 (2001).
[5] V. Rodrigues and D. Ugarte, Phys. Status Solidi (b) **230**, 475 (2002).
[6] G. Rubio, N. Agraït, and S. Vieira, Phys. Rev. Lett. **76**, 2302 (1996).
[7] A. Stalder and U. Dürig, Appl. Phys. Lett. **68**, 637 (1996).
[8] C. Untiedt, G. Rubio, S. Vieira, and N. Agraït, Phys. Rev. B **56**, 2154 (1997).
[9] A. I. Yanson, I. K. Yanson, and J. M. van Ruitenbeek, Nature (London) **400**, 144 (1999).
[10] A. I. Yanson, I. K. Yanson, and J. M. van Ruitenbeek, Phys. Rev. Lett. **84**, 5832 (2000).
[11] U. Landman, W. D. Luedtke, N. A. Burnham, and R. J. Colton, Science **248**, 454 (1990).
[12] T. N. Todorov and A. P. Sutton, Phys. Rev. B **54**, 14 234 (1996).
[13] M. R. Sørensen, M. Brandbyge, and K. W. Jacobsen, Phys. Rev. B **57**, 3283 (1998).
[14] O. Gülseren, F. Ecrolessi, and E. Tosatti, Phys. Rev. Lett. **80**, 3775 (1998).
[15] S. Chandrasekhar, *Hydrodynamic and Hydromagnetic Stability* (Dover, New York, 1981), pp. 515–574.
[16] H. Hakkinen, R. Barnett, A. Scherbakov, and U. Landman, J. Phys. Chem. B **104**, 9063 (2000).
[17] S. Bahn and K. Jacobsen, Phys. Rev. Lett. **87**, 266101 (2001).
[18] C. A. Stafford, D. Baeriswyl, and J. Bürki, Phys. Rev. Lett. **79**, 2863 (1997).
[19] C. A. Stafford, F. Kassubek, J. Bürki, and H. Grabert, Phys. Rev. Lett. **83**, 4836 (1999).
[20] F. Kassubek, C. A. Stafford, H. Grabert, and R. E. Goldstein, Nonlinearity **14**, 167 (2001).
[21] C.-H. Zhang, F. Kassubek, and C. A. Stafford, Phys. Rev. B **68**, 165414 (2003).
[22] See EPAPS Document No. E-PRLTAO-91-071401 for movies of the simulations. A direct link to this document may be found in the online article's HTML reference section. The document may also be reached via the EPAPS homepage (http://www. aip.org/pubservs/epaps.html) or from ftp.aip.org in the directory /epaps/. See the EPAPS homepage for more information.
[23] The locality of the semiclassical functional, Eq. (1), suppresses the dependence on boundary conditions.
[24] D. F. Urban, J. Bürki, C.-H. Zhang, C. A. Stafford, and H. Grabert (to be published).
[25] V. M. Strutinsky, Nucl. Phys. **A122**, 1 (1968).
[26] M. Brack and R. K. Bhaduri, *Semiclassical Physics* (Addison-Wesley, Reading, MA, 1997), and references therein.
[27] The value $\sigma = \varepsilon_F k_F^2/80\pi$ was used [19] to model alkali metals. For noble metals, σ is roughly twice as large.
[28] C. Yannouleas and U. Landman, Phys. Rev. B **51**, 1902 (1995).
[29] D. Ullmo, M. Grinberg, and S. Tomsovic, Phys. Rev. E **54**, 136 (1996).
[30] S. C. Creagh, Ann. Phys. (N.Y.) **248**, 60 (1996).
[31] B. D. Coleman, R. S. Falk, and M. Moakher, Physica (Amsterdam) **89D**, 123 (1995).
[32] J. Eggers, Phys. Rev. Lett. **80**, 2634 (1998).
[33] A. J. Bernoff, A. L. Bertozzi, and T. P. Witelski, J. Stat. Phys. **93**, 725 (1998).
[34] D. Zhang, T. Powers, R. Goldstein, and H. Stone, Phys. Fluids **10**, 1052 (1998).
[35] R. Bar-Ziv and E. Moses, Phys. Rev. Lett. **73**, 1392 (1994).